Synthesis of 2-(*n*-(*N*,*N*,*N*-trimethyl)-*n*-alkyl)-5-alkylfuryl halides Useful probes for studying singlet oxygen dynamics and equilibria in microcompartmentalized systems

Fernando Castañeda, Antonio L. Zanocco, Mónica Meléndrez, Germán Günther, Else Lemp*

Departamento de Química Orgánica y Fisicoquímica, Facultad de Ciencias Químicas y Farmacéuticas, Universidad de Chile, Olivos 1007, Casilla 233, Santiago, Chile

Abstract

Three lipid-soluble furan derivatives, 2,5-disubstituted with different *n*-alkyl chains, and a terminal trimethylammonium group were obtained by reaction of a metalated monoalkylfuran with alkyl dihalides under conditions of thermodynamic control and subsequent reaction with gaseous trimethylamine. These compounds are useful probes for studying singlet oxygen dynamics and equilibria in microcompartmentalized systems because they react very rapidly with singlet oxygen, physical quenching can be neglected, and medium effects on reactivity are small. Location of the probe, completely incorporated in the lipidic bilayer, is predictable and controllable from structural modifications and the small reactive moiety does not modify significantly the vesicle chain packing. Steady-state and time-resolved kinetics employing 2-(4-(*N*,*N*,*N*-trimethyl)-butyl)-5-dodecylfuryl bromide to monitoring singlet oxygen give a value of 0.27 for the singlet oxygen partitioning constant between the lipidic and aqueous pseudophases of 10 mM large unilamellar dioctadecyldimethylammonium chloride (DODAC) vesicles. The steady-state singlet oxygen concentration, sensed by this furan derivative in the microphase, was 2.7×10^{-11} M.

Keywords: Singlet oxygen; Furan derivatives; DODAC vesicles; Singlet oxygen partition constant; Time resolved kinetics

1. Introduction

Singlet molecular oxygen, $O_2(^1\Delta_g)$, reactions are important in biological systems, where they have important deleterious and/or beneficial roles, e.g., in the photo-induced damage of tissues and the photo-dynamic therapy of cancer [1–3]. Evaluation and analysis of singlet oxygen mediated chemical processes in biological systems require an understanding of its reactivity towards different acceptors present in very complex organizations. A critical characteristic of biological systems is their microheterogeneity, consequently, gradients can occur in both the local singlet oxygen concentration and its reactivity. The use of fast response detectors with near-IR sensitivity allows direct detection of $O_2(^1\Delta_g)$, by analyzing its weak emission at 1270 nm in both laser pulsed flash photolysis and steady-state experiments [4–6]. This method is very important for the analysis of $O_2(^1\Delta_g)$ in biological systems. With this technique, Khan et al. [7] detected, for the first time, $O_2(^1\Delta_g)$ emission in an enzymatic reaction. However, employment of this technique in biological systems has serious limitations: (a) during the past 20 years, the 1270 nm singlet oxygen luminescence has been detected mainly with cryogenic germanium diodes, the sensitivity of which, due to the low $O_2(^1\Delta_g)$ lifetime in water (3–4 μs) [8,9], is often insufficient to provide quantitative information in systems with high water content such as protein solutions or membrane suspensions; (b) the $O_2(^1\Delta_g)$ lifetime determined in biological media is averaged over many different deactivation processes. Even for the most simple experimental setup that mimics a biological system, i.e., a micellar solution in absence of quencher, the two pseudophase model [10], predicts that the observed overall decay rate constant depends on the partition constant of singlet oxygen between the two pseudophases, the volume of the each pseudophase and the decay rate constants of $O_2(^1\Delta_g)$ in both the aqueous and micellar regions. In the presence of singlet oxygen quenchers, even where the singlet oxygen equilibrium distribution is maintained, $O_2(^1\Delta_g)$ lifetime determinations as well as steady-state measurements, provide only values of the product of the quenching rate constant in a given pseudophase and the singlet oxygen partitioning constant, averaged over all the pseudophases [11]; (c) time-resolved methods are not currently available

* Corresponding author. Tel.: +56 2 6782877; fax: +56 2 6782868.
E-mail address: elemp@ciq.uchile.cl (E. Lemp).

in many laboratories. These limitations enable chemical trapping methods with well designed water-soluble and/or lipid-soluble singlet oxygen acceptors to be valuable tools in improving understanding of singlet oxygen behavior in microheterogeneous systems. The measurement of $O_2(^1\Delta_g)$ concentration in the aqueous pseudophase of these systems by using acceptors or quenchers is difficult because of the low water solubility of more reactive molecules [12,13]. Most successful compounds employed in these experiments include water-soluble anthracene and diphenylisobenzofuran derivatives [14,15]. Therefore, it is interesting to study the influence of lipid bilayers on the reactivity of the singlet oxygen acceptors incorporated in them, as well as the relationship between acceptor localization and the eventual protective effect of the microenvironment. The ability of singlet oxygen to permeate lipid bilayers can be studied by employing a water-soluble acceptor, which quenches with zero-order kinetics of all the $O_2(^1\Delta_g)$ entering or leaving the bilayer [15]. Alternatively, a highly efficient lipid-soluble singlet oxygen quencher, anchored to the water-lipidic bilayer interphase by means of a charged head group, could be a valuable probe to study singlet oxygen dynamics and estimate steady-state singlet oxygen concentrations at different depths in the bilayer, if there are appropriate spacers between the charged head group and the reactive moiety. One of the most reactive singlet oxygen acceptors in organic solvents is 2,5-dimethylfuran (2,5-DMF) [16]. Its sensitized oxygenation gives a relatively stable ozonide by [4 + 2] cycloaddition of $O_2(^1\Delta_g)$ to the diene system [17,18]. Thermal reactions of the endoperoxide do not interfere with singlet oxygen quenching [16]. Because 2,5-DMF consumption in organic solvents can easily be followed by gas chromatography, it has been frequently employed in actinometry to measure the reactivity of other molecules towards singlet oxygen [19]. Also, singlet oxygen quenching rate constants by 2,5-DMF are practically solvent independent, a critical characteristic of probes for measurements of singlet oxygen distribution between the external solvent and the microphase [11].

In order to apply the well-known ability of 2,5-DMF and its derivatives as singlet oxygen acceptors, and, at the same time, to extend their use to lipidic bilayers, we report here syntheses of three lipid-soluble DMF derivatives, 2,5-disubstituted with alkyl chains of different length and including a terminal trimethylammonium head group in one chain. We also include preliminary measurements of the reactivity of these molecules towards singlet oxygen that show their use in evaluating singlet oxygen behavior in microheterogeneous systems.

2. Experimental details

2.1. General

Melting points (not corrected) were determined on a modified Koffler or on a Electrothermal 9200 apparatus. NMR spectra were performed in a Bruker DRX-300 spectrometer. Chemical shifts are referred to internal tetramethylsilane (TMS). Elemental analyses were obtained in a Fisons EA-1108 instrument. IR spectra were obtained on a Fourier transform Bruker IFS-56 spectrometer. UV–vis measurements were made in a Unicam UV-4 spectrophotometer. A Fisons MD-800 GC-MS system with a Hewlett Packard Ultra-2 capillary column (25 m) was used to obtain electron impact mass spectra. All spectroscopic measurements were performed at room temperature.

2.2. Materials

All solvents used in the syntheses and spectroscopic and kinetic measurements were of reagent grade, spectroscopic or HPLC quality, and when necessary were purified by the usual procedures [20]. Furan (Merck) was distilled before use, and stored at low temperature under argon atmosphere in the dark. Tetraphenylporphyrine (TPP), Methylene Blue (MB), and 1,3-diphenylisobenzofurane (DPBF) (Aldrich) were used as received. Dioctadecyldimethyl ammonium chloride (DODAC) (Herga Ind.) was purified as described elsewhere [21]. The concentration of *n*-butyl lithium (Merck) was determined by employing the double titration method with benzyl chloride [22]. Dodecyl and hexyl iodide were synthesized as described previously [23]. 1,12-Dibromododecane and 1,4-dibromobutane (Aldrich) were used as received.

2.3. Methods

Time resolved luminescence measurements were carried out in 0.5 cm path fluorescence cells at 20 °C. TPP was excited by the second harmonic (532 nm, ca. 9 mJ/pulse) of a 6-ns light pulse of a Quantel Brilliant Q-Switched Nd:YAG laser. When MB was used as the sensitizer samples were excited with the 500-ps light pulse of a PTI model PL-202 dye laser (666 nm, ca. 200 μJ/pulse). A PTI model PL-2300 nitrogen laser was employed to pump the dye laser. A liquid-nitrogen cooled North Coast model EO-817P germanium photodiode detector with a built-in preamplifier was used to detect infrared radiation from the cell. The detector was at a right-angle to the cell. An interference filter (1270 nm, Spectrogon US, Inc.) and a cut-off filter (995 nm, Andover Corp.) were the only elements between the cell face and the diode cover plate. Preamplifier output was fed into the 1 MΩ input of a digitizing oscilloscope Hewlett Packard model 54540-A. Computerized experiment control, data acquisition and analysis were performed with LabView based software developed in our laboratory.

Chemical reaction rate constants were determined in ethanol and 10 mM DODAC vesicular solutions using a 10 mL double wall cell, light-protected by black paint. A centered window allowed irradiation with light of a given wavelength using Schott cut-off filters. Circulating

water maintained the cell temperature at 20 ± 0.5 °C. The irradiation of the sensitizer, MB, was performed with a visible, 200 W, Par lamp. A Waters 600 liquid chromatograph equipped with a PDA detector Waters 996 and a Waters Delta Pack C-4 (3.9 × 150 mm) HPLC column was used to monitor furan derivative consumption. 1,3-Diphenylisobenzofurane was used as actinometer. Fresh 1,3-diphenylisobenzofuran solutions prepared in a dark room and appropriate cut-off filters were used. Autooxidation of this compound, followed by UV–vis spectrophotometry, was <1% under our experimental conditions.

Large unilamellar liposomes of dioctadecyldimethylammonium chloride, DODAC LUVs, were obtained by controlled injection of a DODAC-chloroform solution (20 mM) into 5 mL D_2O (Aldrich) at 75 ± 0.5 °C, according to the procedure previously described [24]. The final concentration was fixed by the amount of injected DODAC–chloroform solution. LUVs with furane derivatives incorporated in the lipidic bilayer were obtained by means of the same procedure but first adding an appropriate amount of the probe to the DODAC–chloroform solution.

2.4. Chemical synthesis

2-Methylfuran (**1**). This was obtained by employing a modification of the Wolff–Kishner method [23]. On a solution of 0.15 mol of KOH in 50 mL of ethylene glycol gently heated, 0.13 mol of hydrazine, 0.15 mol of KOH, 0.13 mol of furfural, and 25 mL of ethylenglycol were added with stirring and the mixture was heated at 90 °C for 1.5 h. Hydrolysis of the hydrazone was complete with addition of 0.45 mol of KOH, stirring overnight at room temperature and heating at 90 °C until nitrogen evolution ended. Distillation of the crude yielded 40% of (**1**), bp 61 °C, ^{1}H NMR ($CDCl_3$): δ: 2.17 (s, 3H); 5.83 (dd, 1H); 6.14 (dd, 1H); 7.14 (dd, 1H).

2-(1-(N,N-Dimethylamine)-methyl)-5-methylfuran (**2**). Typically, the product of the reaction of 0.17 mol of acetic acid, 0.06 mol of 40% aqueous dimethylamine, 0.06 mol of 35% aqueous formaldehyde, and 0.05 mol of 2-methylfuran was worked up by a standard procedure [25] yielding 82% of (**2**), bp 50 °C (10 mmHg). ^{1}H NMR ($CDCl_3$): δ: 2.16 (s, 3H); 2.19 (s, 3H); 3.30 (s, 2H); 5.79 (dd, 1H, $J = 0.77$ Hz; $J = 2.83$ Hz); 5.97 (d, ^{1}H, $J = 2.97$ Hz).

2.4.1. General procedure for furan monoalkylation [26]

Dry THF (100 mL) was cooled to −20 °C in a 250-mL two-necked flask equipped with a reflux condenser, a constant pressure dropping funnel, and a magnetic stirrer, and 0.06 mol of *n*-butyl lithium in *n*-hexane was added with stirring under argon. Freshly distilled furan (0.066 mol) was added, dropwise, into the butyl lithium solution. After 4 h, 0.054 mol of alkyl bromide was added with vigorous stirring and the mixture was left overnight at room temperature. The solution was poured onto 200 g of ice and was extracted with diethyl ether. The extract was dried over magnesium sulfate and the solvent was evaporated under reduced pressure. Distillation of the residue gave 2-alkylfurans.

2-Dodecylfuran (**3**). This compound was prepared in 77% yield from l-iodododecane as described, bp 156–158 °C (15 mmHg); $n_D^{20} = 1.458$; ^{1}H NMR (CCl_4): δ: 0.88 (t, 3H, $J = 6.7$ Hz); 1.27 (m, 18H); 1.61 (t, 2H, $J = 7.2$ Hz); 2.57 (t, 2H, $J = 7.5$ Hz); 5.85 (d, 1H, $J = 3.1$ Hz); 6.14 (dd, 1H, $J = 3.0$ Hz, $J = 2.0$ Hz); 7.17 (d, 1H, $J = 1.1$ Hz). IR (KBr, ν, cm^{-1}): 2924; 2854; 1596; 1463; 1147; 1007; 794; 725. MS *m/e*: 236(M^+), 237 (M + 1).

2-n-Hexylfuran (**4**). As for the preparation of **3**, l-iodohexane yielded 74% of (**4**), bp 72–74 °C (18 mmHg); n_D^{20}: 1.453. ^{1}H NMR ($CDCl_3$): δ: 0.81 (t, 3H, $J = 6.8$ Hz); 1.25 (m, 6H); 1.55 (m, 2H); 2.53 (t, 2H, $J = 7.6$ Hz); 5.88 (d, 1H, $J = 3.1$ Hz); 6.19 (dd, 1H $J = 3.0$ Hz, $J = 2.0$); 7.20 (d, 1H, $J = 1.8$ Hz). IR (KBr, ν, cm^{-1}): 2960; 2930; 2856; 1596; 1507; 1464; 1146; 1008; 923; 795; 726. MS *m/e*: 152 (M^+), 153 (M + 1).

2.4.2. General procedure for the synthesis of 2-(n-bromo-n-alkyl)-5-alkylfuran

Typically, 0.02 mol of 5-alkyl-2-furfuryl lithium was prepared in dry THF by adding freshly distilled 2-alkylfuran (0.22 mol) to *n*-butyl lithium (0.2 mol) as described for monoalkylation. The lithium salt solution (below −20 °C) was transferred to a double-wall constant pressure dropping funnel cooled with dry ice-acetone and was added dropwise into a solution of the dialkyl bromide (0.02 mol) in 2 mL of THF kept below −20 °C. After 3 h, cooling was removed and the mixture was stirred overnight at room temperature. Working up was as described for monoalkylation and distillation of the residue afforded the crude product containing a small amount of dimeric undesirable by-product. Careful distillation was required to afford 2-(*n*-bromo-*n*-alkyl)-5-alkylfuran.

2-(4-Bromobutyl)-5-dodecylfuran (**5**). This compound was prepared in 59% yield from 1,4-dibromobutane according to the already described procedure, bp 196–200 °C (3 mmHg). ^{1}H NMR ($CDCl_3$): δ: 0.88 (t, 3H, $J = 6.7$ Hz); 1.27 (m, 18H); 1.59 (m, 2H,); 1.77 (m, 2H); 1.89 (m, 2H); 2.52 (t, 2H, $J = 7.5$ Hz); 2.57 (t, 2H, $J = 7.1$ Hz); 3.35 (t, 2H, $J = 6{,}6$ Hz); 5,74 (dd, 2H, $J = 3.0$ Hz). IR (KBr, ν, cm^{-1}): 2959; 2921; 2852; 1613; 1566; 1463; 1010; 780; 722; 564 (st C–Br). MS *m/e*: 370 (M^+), 372 (M + 2).

2-(12-Bromododecyl)-5-hexylfuran (**6**). In a reaction similar to that of **5**, 1,12-dibromododecane yielded 45% of (**6**), bp 240–250 °C (3 mmHg). ^{1}H NMR ($CDCl_3$): δ: 0.86 (t, 3H, $J = 6.6$ Hz); 1.39 (m, 22H); 1.58 (m, 4H); 1.83 (m, 2H); 2.53 (t, 4H, $J = 4.0$ Hz); 3.38 (t, 2H, $J = 6.7$ Hz); 5.81 (s, 2H). MS *m/e*: 398 (M^+), 400 (M + 2).

2.4.3. General procedure for the synthesis of 2-(n-(N,N,N-Trimethyl)-n-alkyl)-5-alkylfuryl halides

Usually, dry gaseous trimethylamine, produced by heating 23% aqueous trimethylamine and dried with a soda lime

trap, was bubbled into 0.007 mol of 2-(*n*-bromo-*n*-alkyl)-5-alkylfuran in 10 mL of dry acetone. After 20 min, a white precipitate was formed. Solvent removal under vacuum and recrystallization from acetone gave the ammonium salt.

2-(4-(N,N,N-Trimethyl)-butyl)-5-dodecylfuryl bromide (DFTA). This compound was prepared in 75% yield from compound **5** following the described procedure, mp 124–130 °C. ^{1}H NMR ($CDCl_3$): δ: 0.81 (t, 3H, $J = 6.7$ Hz); 1.19 (m, 18H); 1.53 (t, 2H); 1.70 (m, 4H); 2.47 (m, 2H, $J = 7.6$ Hz); 2.61 (t, 2H, $J = 6.7$); 3.39 (s, 9H); 3.53 (t, 2H, $J = 8.1$ Hz); 5.81 (dd, 2H, $J = 3.0$ Hz). Elem. anal.: calc. %C: 64.20; %H: 10.24; %N: 3.26; exp. %C: 63,60; %H: 10.01; %N: 3.48.

2-(12-(N,N,N-Trimethyl)-dodecyl)-5-hexylfuryl bromide (HFDA). Following the procedure for preparation of DFTA, *2-(10-bromododecyl)-5-hexylfuran* (**6**) yielded 68% of HFDA, mp 210–215 °C with dec. ^{1}H NMR ($CDCl_3$): δ: 0.89 (t, 3H, $J = 6.7$ Hz); 1.31 (m, 22H); 1.61 (t, 4H); 1.73 (m, 2H); 2.57 (t, 4H, $J = 7.8$); 3.49 (s, 9H); 3.58 (t, 2H); 5.85 (s, 2H). Elem. anal.: calc. %C: 65,50; %H: 10,48; %N: 3,06; exp. %C: 65.38; %H: 10.65; %N: 3.29.

2-(1-(N,N,N-Trimethylamine)-methyl)-5-methylfuran iodide (MFMA). A mixture of 0.27 mol of methyl iodide and 0.04 mol of 2-(1-(*N,N*-dimethylamine)-methyl)-5-methylfuran (**2**) in 15 mL of dry acetone was stirred under argon overnight at room temperature. Isolation of the white precipitate and recristallization yielded 81% of MFMA, mp 160–162 °C with dec. ^{1}H NMR ($CDCl_3$): δ: 2.24 (s, 3H); 3.37 (s, 9H); 4.88 (s, 2H); 6.00 (s, 1H); 6.79 (s, 1H). Elem. anal.: calc. %C: 38.45; %H: 5.70; %N: 4.98; exp. %C: 38.28; %H: 5.93; %N: 5.14.

3. Results and discussion

3.1. Synthesis of 2-(n-(N,N,N-trimethyl)-n-alkyl)-5-alkylfuryl halides

Structure of compounds synthesized in this work are shown in Fig. 1. DFTA and HFDA were obtained according to Scheme 1, whereas compound MFMA was obtained by using conventional methods [23,25].

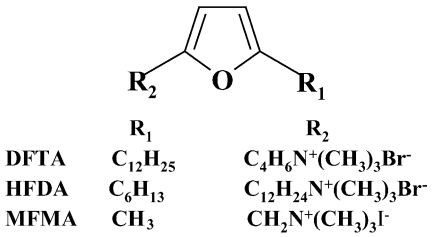

	R_1	R_2
DFTA	$C_{12}H_{25}$	$C_4H_6N^+(CH_3)_3Br^-$
HFDA	C_6H_{13}	$C_{12}H_{24}N^+(CH_3)_3Br^-$
MFMA	CH_3	$CH_2N^+(CH_3)_3I^-$

Fig. 1. Structures of 2-(*n*-(*N,N,N*-trimethyl)-*n*-alkyl)-5-alkylfuryl halides.

Reactions of lithium salts of furan, pyrroles, thiophene, and their alkyl derivatives with alkyl halides have been previously described [27,28]. However, the only example of reactions of this type of lithium salts with alkyl dihalides has been reported by Catoni et al. [29]. Reactions of alkylfuran lithium salt derivatives with alkyl dihalides require a careful thermodynamic control to avoid formation of dimeric by-products as shown in Scheme 2. The inverse addition technique, that is, addition of the metalated alkylfuran to a concentrated solution of the alkyl dihalide maintained at very low temperature, allows rigorous thermodynamic control, diminishing by-product formation and increasing reaction yield. All compounds synthesized were characterized by conventional spectroscopic and/or analytical techniques. Further details are given in the experimental section.

3.2. Preliminary kinetic study of 2-(n-(N,N,N-trimethyl)-n-alkyl)-5-alkylfuryl halides as singlet oxygen probes

In homogeneous media, reaction of singlet oxygen with a target molecule, Q, involves physical (deactivation) and/or chemical (reactive) processes. The situation can be represented in terms of a simple mechanism as shown in Scheme 3:

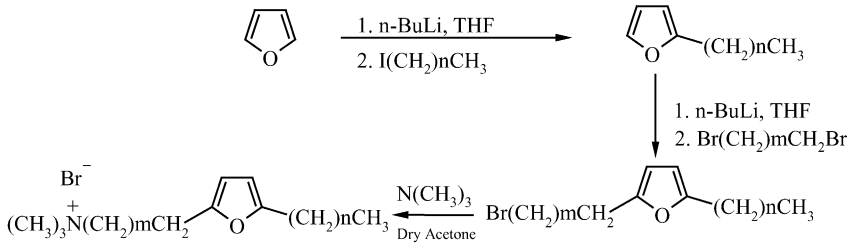

	n	m
DFTA	11	3
HFDA	5	11

Scheme 1.

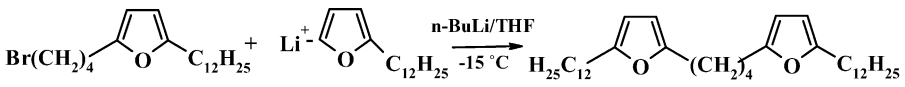

Scheme 2.

$$^1O_2 \xrightarrow{k_d} O_2 \quad (1)$$

$$^1O_2 + Q \xrightarrow{k_{ph}} Q + O_2 \quad (2)$$

$$^1O_2 + Q \xrightarrow{k_r} \text{Products} \quad (3)$$

Scheme 3.

where k_d is the solvent dependent decay rate constant of singlet oxygen that determines its unperturbed lifetime ($\tau_o = 1/k_d$), k_{ph} represents the second-order rate constant of physical deactivation, and k_r is the second-order rate constant of the reactive pathway. In the presence of Q, the singlet oxygen lifetime, τ, is given by:

$$\frac{1}{\tau} = k_D = k_d + k_T[Q] \quad (4)$$

where k_T is the rate constant of the whole quenching process ($k_T = k_{ph} + k_r$). Evaluation of the singlet oxygen lifetime at different concentrations of Q then allows determination of k_T. This type of experiment can be carried out by following the decay of $O_2(^1\Delta_g)$ luminescence, measured at 1270 nm, and provides the most reliable value of the total deactivation rate constant.

The values of total (physical and chemical) quenching rate constants, k_T, for the reaction of $O_2(^1\Delta_g)$ with furan derivatives in several media, were obtained from the experimentally measured first-order decays of singlet oxygen in the absence (k_d) and presence of the furan derivative (k_D) according to Eq. (4).

Fig. 2 shows a typical Stern–Volmer plot obtained for singlet oxygen quenching with DFTA in acetonitrile. The triplet decay of the sensitizer (TPP or MB) was not affected by the addition of furan derivatives even at concentrations higher than those used to quench the excited oxygen, and linear plots of k_D versus substrate concentrations were obtained in all the homogeneous media employed. The intercepts of these plots correspond to the singlet oxygen lifetime in the solvent employed. In all the experiments these values match

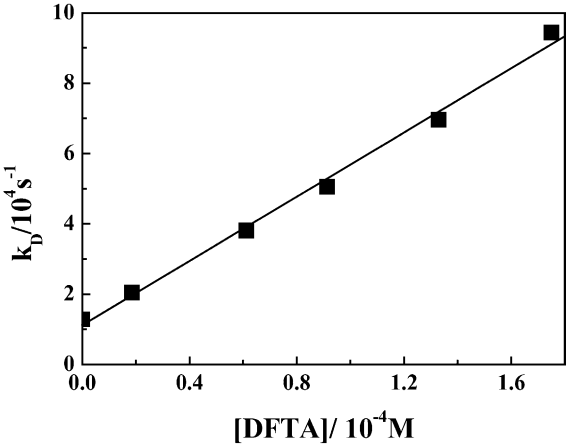

Fig. 2. Stern–Volmer plot for singlet oxygen deactivation by DFTA in acetonitrile.

very closely singlet oxygen lifetimes determined independently in experiments performed in our laboratory [30–32].

Scheme 4 shows a physical model with the minimum requirements for explaining singlet oxygen decay and reactions in microheterogeneous systems comprising micelles, reverse micelles, vesicles, and simple single membrane biological systems (such as red blood cell ghosts or microsomes) [11]. This scheme includes, as pseudophases, the aqueous external solvent and the vesicle or membrane bilayer neglecting the inner water pool because of its small contribution to the total aqueous volume. In addition, in our experiments with vesicular solutions, singlet oxygen was generated only in the external aqueous pseudophase because the sensitizer (MB) was added to DODAC vesicular solutions just before measurements and in this system MB permeation through the bilayer is negligible at room temperature (20 ± 2 °C) [33]. Also, due to the structural similarity of DFTA and HFDA with the anthracene and pyrene derivatives, currently employed as fluorescent probes in vesicles of synthetic and natural surfactants [34–38], we consider that DFTA and HFDA are located exclusively in the lipidic pseudophase. The trimethylammonium head group and the

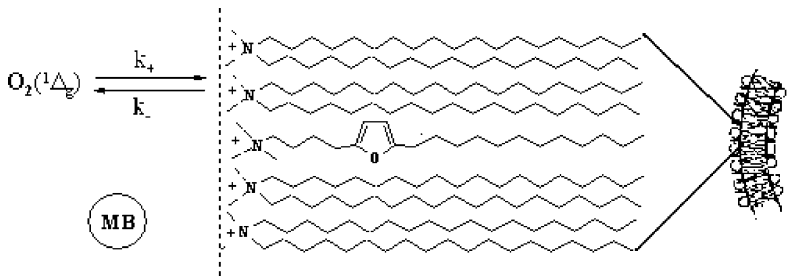

Scheme 4.

length of the tether alkyl group locates the reactive furan moiety depth in the vesicle bilayer on the assumption that alkyl groups are extended. In more complex models both oxygen generation and/or interaction with the target molecule could take place also at the water–lipid interface. According to the simpler model [10] the k_D value measured in time resolved experiments with furan derivatives anchored to the bilayer of DOCAC vesicles, is given by:

$$k_D = k_d + (1 - f)k_T^L[Q]^L \quad (5)$$

where f is the fraction of singlet oxygen in the aqueous pseudophase, k_T^L is the total quenching rate constant in the bilayer and $[Q]^L$ is the local quencher concentration expressed in moles L^{-1} of lipidic bilayer. If K, the singlet oxygen partitioning constant between the bilayer and the aqueous pseudophase, is defined as:

$$K = \frac{[O_2(^1\Delta_g)]^L}{[O_2(^1\Delta_g)]^W} \quad (6)$$

where $[O_2(^1\Delta_g)]^L$ and $[O_2(^1\Delta_g)]^W$ are the singlet oxygen concentrations in the bilayer and the external solvent, respectively. From Eqs. (5) and (6) it is found that:

$$k_D = k_d + K\,k_T^L[Q] \quad (7)$$

with [Q] being the analytical quencher concentration. Eq. (7) shows that the slopes of Stern–Volmer plots in a system described in terms of the two pseudophase model then correspond to an apparent second order rate constant:

$$k_{app} = K\,k_T^L \quad (8)$$

Fig. 3 shows the decay of singlet oxygen in a DODAC vesicular solution, in the absence and with added 2.5×10^{-5} M DFTA. The signal have good signal/noise. The complexities normally observed in this type of experiment, due to the low singlet oxygen lifetime in aqueous media,

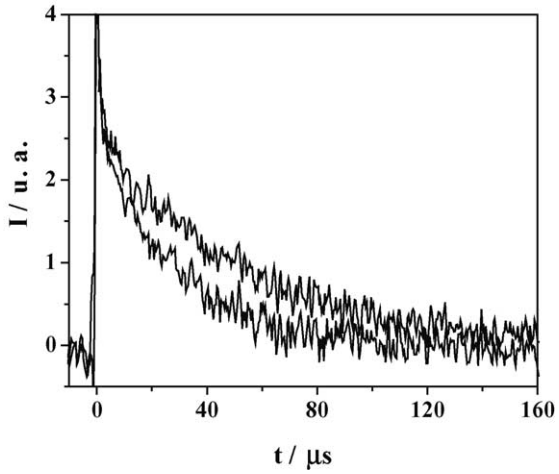

Fig. 3. Singlet oxygen phosphorescence decay at 1270 nm in 10 mM DODAC vesicles, following dye laser excitation of MB at 666 nm in the absence (upper decay) and in the presence (lower decay) of 2.5×10^{-5} M of DFTA.

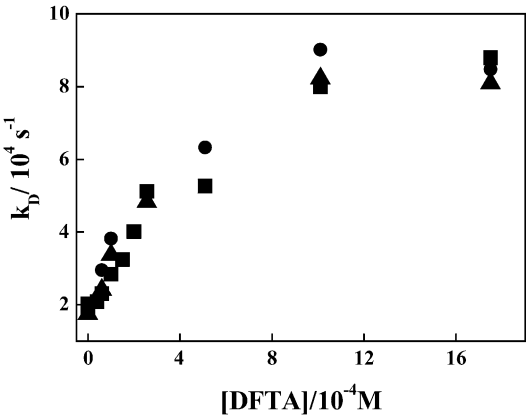

Fig. 4. Stern–Volmer type plot for singlet oxygen deactivation by DFTA in 10 mM DODAC vesicles. Measured freshly ■, after one day ●, after two days ▲ .

were avoided by using deuterated water [39,40] in preparing DODAC vesicles. Decays of Fig. 3 show that $O_2(^1\Delta_g)$ lifetimes diminish in the presence of DFTA anchored to the bilayer. Noting that concentration of the hydrophobic quencher in water will be negligible.

Stern–Volmer plots obtained from the singlet oxygen luminescence decays employing furan derivatives anchored to the lipidic bilayer as quenchers are included in Fig. 4. Dependences of k_D on the quencher concentration do not follow a linear behavior as observed in homogeneous solution, but k_D increases linearly at low concentrations of furan derivative and reaches a practically constant value at higher concentrations. This behavior, typical of microheterogeneous systems has been reported by Nonell et al. [41] for small dipalmitoyl phosphatidylcholine unilamellar vesicles, DPPC SUVs, and can be understood in terms of bilayer saturation. At high "local" concentrations the probe traps all the singlet oxygen reaching the vesicle. In this situation, singlet oxygen lifetime in the lipidic pseudophase is very short due to the efficient quenching process promoted by the furan derivative anchored to the bilayer and the decay rate constant, k_D, fits Eq. (9):

$$k_D = k_d + k_{exch} \quad (9)$$

where k_d is the rate constant associated with the $O_2(^1\Delta_g)$ solvent promoted decay in the pseudophase in which the singlet oxygen lifetime is measurable, and k_{exch} is the rate constant for the singlet oxygen exchange between the aqueous and lipidic pseudophases. The plot of Fig. 4 gives a $k_D = 8.4 \times 10^4\ s^{-1}$, from which the entrance rate constant is, $k_+ = 1.5 \times 10^{13}\ M^{-1}\ s^{-1}$, considering a DODAC LUVs concentration of 2.6×10^{-9} M [42] and a singlet oxygen average lifetime in D_2O of 58 μs from a large set of measurements performed in our laboratory (data not published). This value of k_+ is larger than that calculated from data of Nonell et al. [41], for DPBF-loaded DPPC SUVs ($k_+ = 2 \times 10^{11}\ M^{-1}\ s^{-1}$) and very close to the value estimated by applying the Smoluchowsky formalism ($1 \times 10^{13}\ M^{-1}\ s^{-1}$).

Table 1
Values of the total rate constants, k_T for reaction of singlet oxygen with furan derivatives in different media

Solvent	$k_T/10^8\ M^{-1}\ s^{-1}$				
	2-Methylfuran[a]	2,5-DMF[b]	DFTA	HFDA	MFMA
n-Hexane	0.25 ± 0.13	2.11 ± 0.08	1.8 ± 0.10	1.91 ± 0.12	–
n-Heptane	–	2.39 ± 0.10	–	–	–
n-Octanol	0.72 ± 0.29	–	–	–	–
n-Hexanol	0.75 ± 0.30	–	–	–	–
Benzene	1.22 ± 0.62	5.06 ± 0.20	2.81 ± 0.11	3.48 ± 0.14	2.60 ± 0.14
Ethyl acetate	0.98 ± 0.51	4.44 ± 0.18	–	–	
Acetonitrile	1.88 ± 1.01	3.39 ± 0.10	4.43 ± 0.38	4.23 ± 0.16	2.06 ± 0.12
Chloroform	–	2.96 ± 0.08	1.86 ± 0.06		–
Acetone	1.39 ± 0.71	4.45 ± 0.18	–	–	–
Methylene dichloride	1.11 ± 0.58	4.02 ± 0.12	–	–	–
Methanol	1.16 ± 0.62	5.33 ± 0.27	–	–	–
Ethanol	0.83 ± 0.54	3.33 ± 0.13	3.45 ± 0.27	3.00 ± 0.09	0.15 ± 0.04
n-Propanol	0.88 ± 0.69	4.18 ± 0.17	–	–	–
Benzyl alcohol	2.41 ± 1.45	7.46 ± 0.30	3.50 ± 0.14	–	–
Dimethylformamide	2.84 ± 1.53	7.94 ± 0.31	–	–	–
Benzonitrile	2.02 ± 1.04	6.50 ± 0.26	–	–	–
Propylencarbonate	2.90 ± 1.62	8.58 ± 0.34	–	–	–
D_2O	–	4.43 ± 0.18	3.59 ± 0.29	3.53 ± 0.13	1.5 ± 0.08
DODAC 10 mM	–	–	4.83 ± 0.21	3.86 ± 0.19	5.77 ± 0.22

[a] From ref. [30].
[b] From ref. [11].

The higher value of k_+ determined for the system studied here can be understood in terms of the larger size of DODAC LUVs compared with DPPC SUVs.

Table 1 summarizes k_T values obtained for several furan derivatives in different media. Values of k_T for singlet oxygen reactions with quenchers anchored to the bilayer in 10 mM DODAC LUVs (bottom file) correspond to k_{app} ofEq. (8) and were calculated at low concentrations of furan derivative, where there is a linear dependence of k_D on the analytical furan derivative concentration. Examination of the data in Table 1 reveals several characteristics associated with the effect of the medium on the reactivity of furan derivatives. Largest dependences were observed for methylfuran, where k_T increases by nearly in a factor of ten when the solvent changes from hexane to dimethylformamide. Also this compound shows the smaller k_T values typical of mono-substituted furans [17]. Furthermore, 2,5-DMF, DFTA, and HFMA show similar quenching rate constants with little solvent dependence. MFMA behaves slightly differently, being less reactive in homogeneous solvents than in DODAC vesicular solutions. These differences can be ascribed to diverse factors. In homogeneous solvents the steric inhibition due to the 2-methylenetrimethylammonium group and its electron withdrawing effect (singlet oxygen is electrophilic) reduces the effectiveness of encounters between $O_2(^1\Delta_g)$ and the furan derivative. In vesicular solutions these unfavorable effects can be overcome by localization of the probe in the vesicle. Due to its structure MFMA could be expected to locate nearly at the interface, where local pH, surface potential, microviscosity, and micropolarity are important in determining reactivity. Further studies of the effect of these factors are being performed.

On the other hand, we determine values of k_r, the reactive rate constant (due to chemical quenching) for reactions of DFTA and HFDA with singlet oxygen in ethanol and 10 mM DODAC vesicular solutions, by following consumption of the furan derivative by HPLC. In these experiments reaction is first-order in furan as shown in Fig. 5. In homogeneous solvents, the slope of the first order-plot, k_{exp}, is:

$$k_{exp} = k_r(Q)[O_2(^1\Delta_g)] \quad (10)$$

where $k_r(Q)$ is the second-order rate constant for the chemical reaction of singlet oxygen with the quencher and $[O_2(^1\Delta_g)]$ is the steady-state singlet oxygen concentration. Employing as actinometer, A, a singlet oxygen quencher with $k_r^{(A)}$ previously measured:

$$k_r(Q) = \frac{k_{exp}(Q)}{k_{exp}(A)} k_r(A) \quad (11)$$

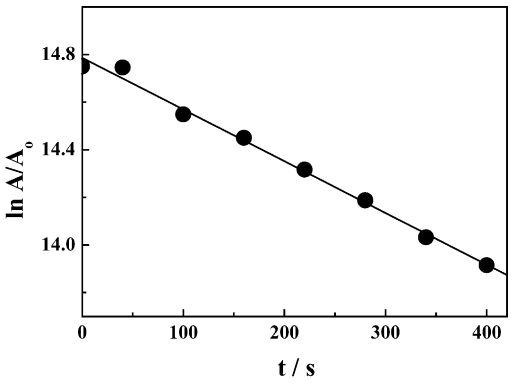

Fig. 5. First-order plot for DFTA reaction with singlet oxygen in 10 mM DODAC vesicular solution.

With diphenylisobenzofuran as actinometer, k_r(DPBF) $= 1.0 \times 10^9\,M^{-1}\,s^{-1}$ [43], we found that k_r(DFTA) and k_r(HFDA) in ethanol are $(3.1 \pm 0.30) \times 10^8\,M^{-1}\,s^{-1}$ and $(2.9 \pm 0.26) \times 10^8\,M^{-1}\,s^{-1}$, respectively. These values are very close to those measured by time resolved methods for these compounds in the same solvent (Table 1). This result indicates that the reaction of singlet oxygen with DFTA and HFDA occurs mainly through the chemical path and in homogeneous solvent $k_T = k_{ph} + k_r \approx k_r$. This result is not novel because it has been reported that furan derivatives quench singlet oxygen only through the chemical pathway to yield endoperoxides, but it is important to show that for these compounds the physical contribution to singlet oxygen quenching is negligible.

According to the two pseudophase model, the slope of the first-order plot, k_{exp}, obtained in steady-state experiments by following the furan consumption in vesicular solutions with furan anchored to the bilayer, is:

$$k_{exp} = k_r^L[O_2(^1\Delta_g)]^{L,F} \tag{12}$$

where k_r^L is the singlet oxygen chemical quenching rate constant in the bilayer and $[O_2(^1\Delta_g)]^{L,F}$ is the singlet oxygen concentration in the probe microenvironment within the bilayer. Only if assumed a homogeneous distribution of singlet oxygen throughout the lipidic pseudophase, $[O_2(^1\Delta_g)]^{L,F} = [O_2(^1\Delta_g)]^L$. Our preliminary results suggest that in vesicular solutions this assumption is not correct.

However, for DFTA, k_T values are relatively solvent independent (Table 1), and the reactive furan group should be located about five methylene group inside the bilayer where the microenvironment should be similar to that of hexane [44], we therefore propose that for DFTA anchored to the bilayer $k_T^L \approx k_r^L \approx k_T^{hexane}$, thus Eqs. (8) and (12) give:

$$K = \frac{k_{app}}{k_T^L} = \frac{k_{app}}{k_T^{hexane}} \tag{13}$$

$$[O_2(^1\Delta_g)]^{L,F} = \frac{k_{exp}}{k_r^L} = \frac{k_{exp}}{k_T^{hexane}} \tag{14}$$

Eqs. (13) and (14) show that the singlet oxygen partitioning constant and the singlet oxygen concentration sensed by DFTA in the bilayer can be evaluated experimentally. Employing the measured values for DFTA we found $K = 0.27$ and $[O_2(^1\Delta_g)]^{L,F} = 2{,}7 \times 10^{-11}$ M. The singlet oxygen partitioning constant and the singlet oxygen concentration in the lipidic bilayer are estimated for the first time in DODAC LUVs.

In conclusion, 2-(*n*-(*N*,*N*,*N*-trimethyl)-*n*-alkyl)-5-alkylfuryl halides are useful probes for studying singlet oxygen dynamics and equilibria in microcompartmentalized systems because they meet all the conditions as actinometers in lipidic microphases: viz., high chemical reactivity with singlet oxygen and physical quenching negligible, complete incorporation in the lipidic microphase, predictable and controllable location of the probes in lipidic bilayers from structural modifications, a small reactive moiety that does not significantly modify vesicular chain packing, and a small reactivity dependence on the media.

Acknowledgements

The financial support from FONDECYT (grant 1030742) is gratefully acknowledged.

References

[1] K. Briviba, L.-O. Klotz, H. Sies, Biol. Chem. 378 (1997) 1259–1265.
[2] L.M. Hultén, M. Holmström, B. Soussi, Free Radic. Biol. Med. 27 (1999) 1203–1207.
[3] M. Tarr, D.P. Valenzeno, Photochem. Photobiol. Sci. 2 (2003) 355–361.
[4] C. Schweitzer, R. Schmidt, Chem. Rev. 103 (2003) 1685–1757.
[5] S. Nonell, S.E. Braslavsky, Methods Enzymol. 319 (2000) 37–49.
[6] E. Oliveros, P. Muraseccosuardi, A.M. Braun, Methods Enzymol. 213 (1992) 420–429.
[7] A.U. Khan, P. Gebauer, L.P. Hager, Proc. Natl. Acad. Sci. USA 80 (1983) 5195.
[8] M.A.J. Rodgers, J. Am. Chem. Soc. 105 (1983) 6201–6205.
[9] A.A. Krasnovsky, S.Yu. Egorov, Biophysics (Engl. Transl.) 28 (1983) 532–534.
[10] P.C. Lee, M.A.J. Rodgers, J. Phys. Chem. 87 (1983) 4894–4898.
[11] E.A. Lissi, E. Lemp, A.L. Zanocco, in: V. Ramamurthy, K.S. Schanze (Eds.), Understanding and Manipulating Excited-States Processes, M. Dekker, New York, 2001, pp. 287–316.
[12] N. Duran, in: W. Adam, G. Cilento (Eds.), Chemical and Biological Generation of Excited States, Academic Press, New York, 1982, p. 345.
[13] C.S. Foote, in: H.H. Wasserman, R.W. Murray (Eds.), Singlet Oxygen, Academic Press, New York, 1979, p. 139.
[14] B.A. Lindig, M.A.J. Rodgers, A.P. Schaap, J. Am. Chem. Soc. 102 (1980) 5590–5593.
[15] F. Amat-Guerri, E. Lemp, E.A. Lissi, F.J. Rodriguez, F.R. Trull, J. Photochem. Photobiol. A Chem. 93 (1996) 49–56.
[16] K. Gollnick, A. Griesbeck, Tetrahedron 41 (1981) 2057–2068.
[17] E.L. Clennan, Tetrahedron 47 (1991) 1343–1382.
[18] E.L. Clennan, M.E. Mehrsheikh-Mahammadi, J. Org. Chem. 49 (1984) 1321–1322.
[19] Y. Usui, K. Kamogawa, Photochem. Photobiol. 19 (1974) 245–247.
[20] K.B. Wiberg, Laboratory Technique in Organic Chemistry, McGraw-Hill, New York, 1960.
[21] M. Barra, C. Bohne, A.L. Zanocco, J.C. Scaiano, Langmuir 8 (1992) 2390–2395.
[22] H. Gilman, A.H. Haubein, J. Am. Chem. Soc. 66 (1944) 1515–1516.
[23] A.I. Vogel, A Textbook of Practical Organic Chemistry Practical Organic Chemistry, third ed., Wiley, London, 1963.
[24] M.V. Encinas, E. Lemp, E.A. Lissi, J. Photochem. Photobiol. B Biol. 3 (1989) 113–122.
[25] H. Gilman, A. H. Batt, Organic Synthesis, vol. VI, second ed., Wiley, New York, 1963, pp. 626–627
[26] E.A. Lissi, M.V. Encinas, F. Castañeda, F.A. Olea, J. Phys. Chem. 84 (1980) 251–255.
[27] G. Büchi, H. Wüest, J. Org. Chem. 31 (1966) 977–978.
[28] C. Galli, G. Illuminati, L. Mandolini, J. Org. Chem. 45 (1980) 311–315.
[29] G. Catoni, C. Galli, L. Mandolini, J. Org. Chem. 45 (1980) 1906–1908.
[30] A.L. Zanocco, G. Günther, E. Lemp, J.R. la Fuente, N. Pizarro, Photochem. Photobiol. 68 (1998) 487–493.

[31] A.L. Zanocco, G. Günther, E. Lemp, J.R. de la Fuente, N. Pizarro, J. Photochem. Photobiol. A Chem. 140 (2001) 109–115.
[32] E. Lemp, A.L. Zanocco, E.A. Lissi, Curr. Org. Chem. 7 (2003) 799–819.
[33] A.L. Zanocco, G. Günther, E. Lemp, E.A. Lissi, J. Chem. Soc. Perkin Trans II (1998) 319–323.
[34] P. Cooper, J.B. Meddings, Biochim. Biophys. Acta 1069 (1991) 151–156.
[35] J. Villalain, M. Prieto, Chem. Phys. Lipids 59 (1991) 9–16.
[36] G.P. L'Heureux, M. Fragata, J. Colloid. Interface Sci. 513 (1987) 117–121.
[37] G.P. L'Heureux, M. Fragata, J. Photochem. Photobiol. B Biol. 3 (1989) 53–63.
[38] M.A. Soto, C.P. Sotomayor, E.A. Lissi, J. Photochem. Photobiol. A Chem. 152 (2002) 79–93.
[39] R.H. Young, D. Brewer, R.A. Keller, J. Am. Chem. Soc. 95 (1973) 375–379.
[40] B.A. Linding, M.A.J. Rodgers, A.P. Schaap, J. Am. Chem. Soc. 102 (1980) 5590–5593.
[41] S. Nonell, S.E. Braslavsky, K. Shaffner, Photochem. Photobiol. 51 (1990) 551–556.
[42] A.M. Carmona Ribeiro, H. Chaimovich, Biochim. Biophys. Acta 733 (1983) 172–179.
[43] M. Nowakowska, J. Chem. Soc. Faraday Trans. 1 (1980) 2119–2126.
[44] S.J. Marrink, J. Phys. Chem. 100 (1996) 16729–16738.